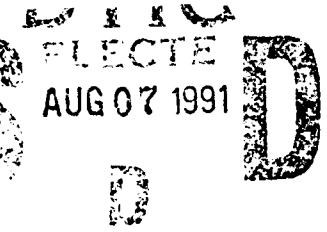

(2)

TRW

Final Report

Phased Array Components for the High Temperature Superconducting Space Experiment (HTSSE)

Contract Number N00014-91-C-2057
TRW Project Number 58212

Prepared for
Naval Center for Space Technology
Naval Research Laboratory
4555 Overlook Ave SW
Washington DC 20375-5000

Prepared by
TRW S&TG
One Space Park
Redondo Beach CA
90278

June 7, 1991

HTSSE Final Report

Table of Contents

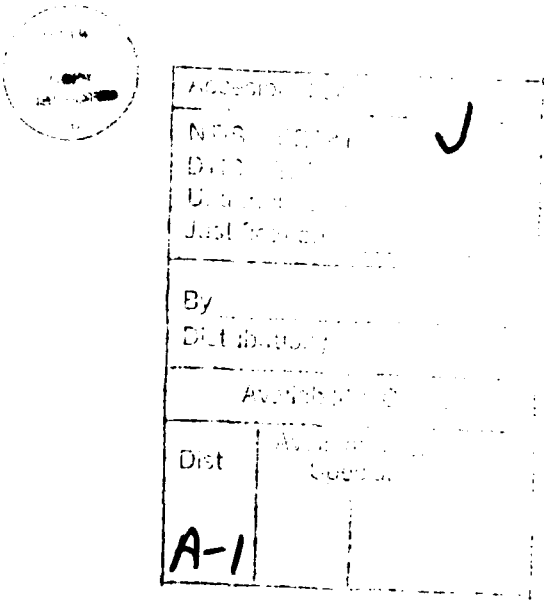

Final Report on Phased Array Components for the High Temperature Superconducting Space Experiment (HTSSE)

Abstract

A new class of X-band phase shifters using the distributed Josephson inductance (DJI) effect were delivered to NRL for the HTS Space Experiment project. Phase shifts were observed above 77 K, and large phase shifts (>60 degrees) were observed at 65 K and below. This narrow-band device was developed as a first step to a broadband device. A total of 40 HTS SQUIDs were successfully integrated into a monolithic circuit. Measurement of the temperature dependance of the Q of a resonator in June 1990 and in February 1991 showed no significant change due to aging.

1.0 Summary of Accomplishments

This program demonstrated a new HTS phase shifter operating at 77 K. Large phase shifts (>60 degrees) were observed at 65 K and below. The phase shifter circuit used a total of 40 engineered HTS SQUIDs in a new design- the distributed Josephson inductance (DJI) phase shifter. The large number of SQUIDs integrated monolithically in each circuit has laid the foundation for a broadband, true time delay phase shifter. These devices are a substantial improvement over the single SQUID phase shifter devices delivered in June 1990.

A total of seven X-band phase shifters were fabricated, and five were delivered to Naval Research Laboratory. The HTS phase shifter consists of a low loss $YBa_2Cu_3O_7$ microstrip resonator with 40 SQUID devices monolithically imbedded into the transmission line. This narrow-band device was developed as a first step to a broadband device.

This program also investigated the effects of aging on an HTS resonator fabricated in June 1990. Measurement of the temperature dependance of the Q in June 1990 and in February 1991 showed no significant change due to aging.

The phase shifters that were fabricated and tested under this program are an early step toward the fabrication of a millimeter-wave phased array receiver. This new method for phase control enables the design of a new class of phased array antennas. A compact, low power, cryocooler can cool a 60 GHz phased array receiver, sketched in Figure 1-1.

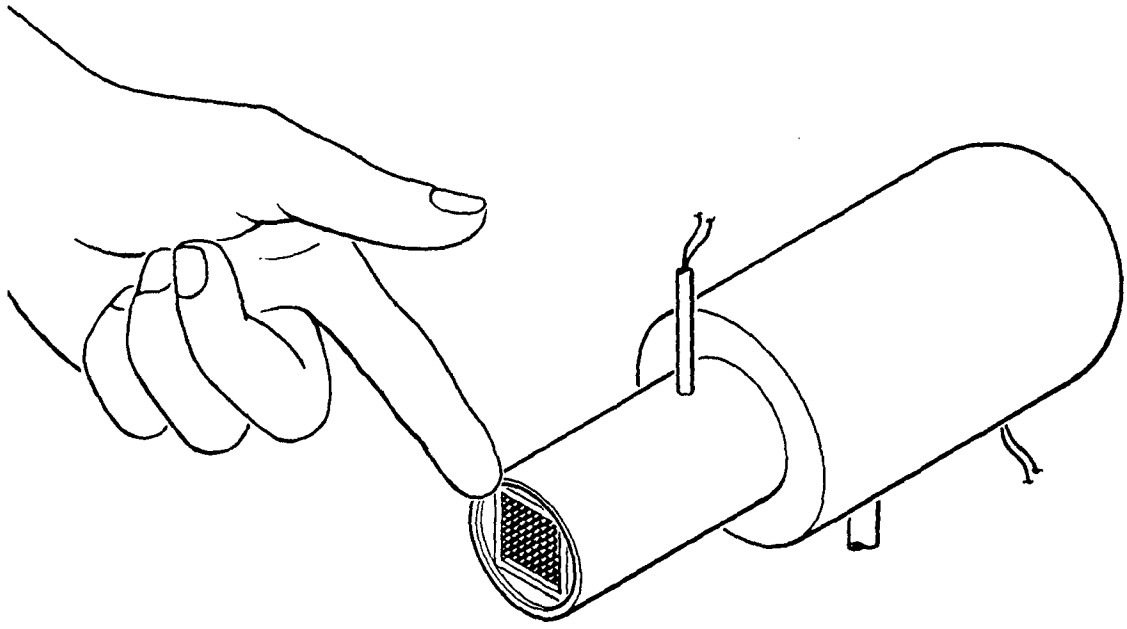

Fig. 1-1 Phased array antenna mounted in a compact cryocooler.

2.0 HTS Phase Shifter Fabrication

The HTSSE phase shifter circuits were fabricated by laser deposition of HTS films on $LaAlO_3$ substrates. A total of 40 HTS step edge SQUIDs were monolithically integrated into an HTS microstrip resonator. An external coil provided phase control. Monolithic implementation of the HTS SQUIDs improved the performance substantially over the phase shifters delivered in June 1990.

2.1 HTS Film Deposition

High quality laser deposited films were used to to make the HTS phase shifter circuits. A high power pulsed laser (shown in Fig. 2.1-1) and a stoichiometric $YBa_2Cu_3O_7$ (YBCO) target deposited films on a heated substrate. Large area coverage was obtained by raster-scanning the substrate past the collimated laser ablation plume.

To obtain SQUID devices, the $LaAlO_3$ substrate was ion milled with step edge patterns prior to film deposition. The next section will describe the YBCO film properties; that section will be followed by a short discussion of the SQUID devices.

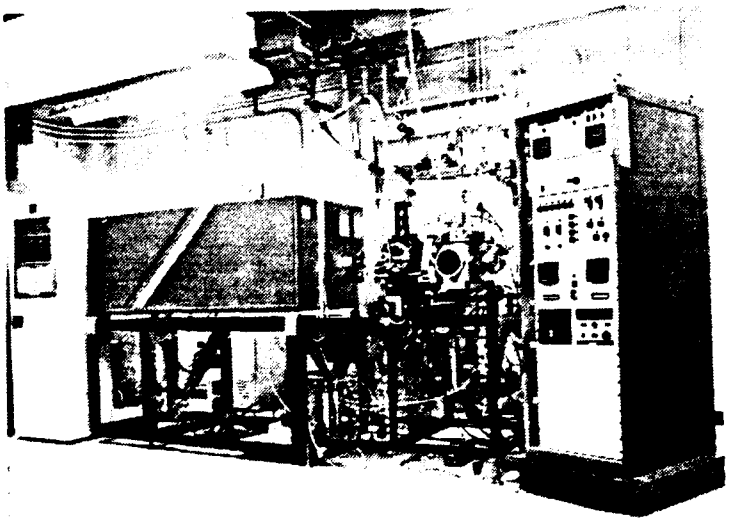

Fig. 2.1 Laser deposition system.

2.2 HTS Film Characterization

High quality YBCO films are routinely deposited in the laser system. The laser deposited films exhibit sharp dc resistance transitions (Tc>91 K), sharp magnetization transitions, low microwave resistance, and high current densities, as shown in Fig. 2.2–1.

Properties of HTS Films made by Pulsed Laser Deposition

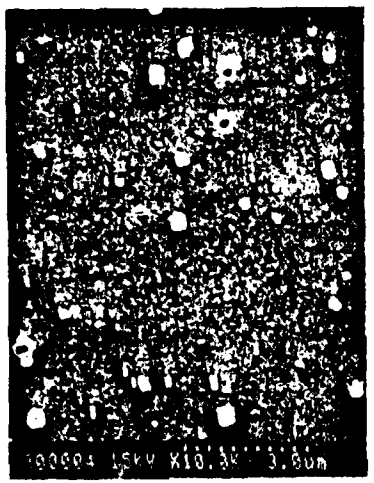

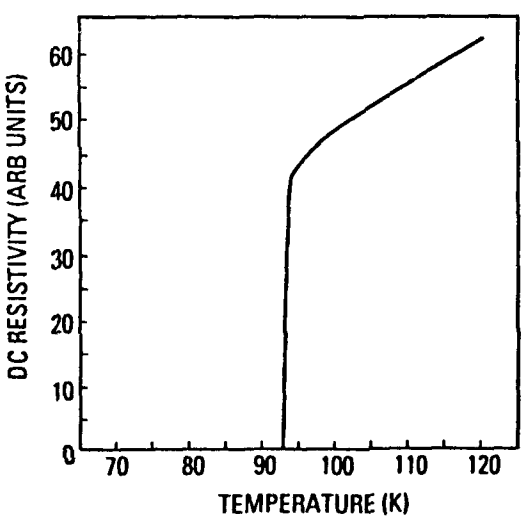

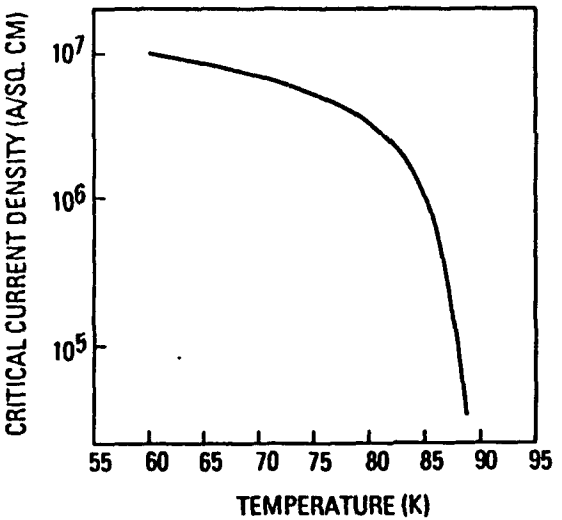

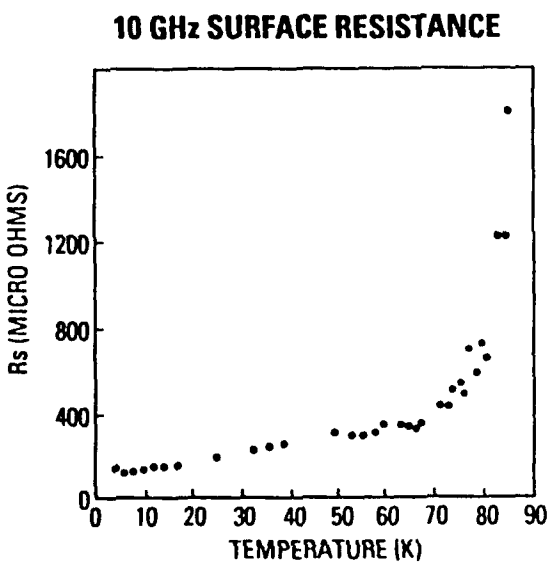

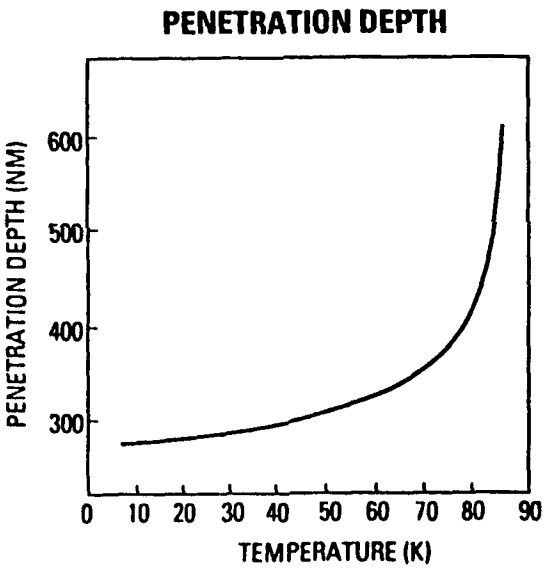

Fig. 2.2-1 Properties of Laser ablated films.

2.3 SQUID Fabrication

Step edge HTS SQUIDs were fabricated by depositing HTS microbridges over a sharp step formed in the $LaAlO_3$ substrate. A 0.15 µm deep trough was ion-milled out of the substrate, and a 0.3 µm thick HTS film was deposited over the step, resulting in an engineered weak link Josephson element. Although there are two step edges in series, only the one with the smaller Ic dominates.

The yield on the chips was very high. Over 90% of the circuits had high Tc values, and all of the circuits demonstrated non-linearities due to SQUID devices. The yield of the SQUIDs could not be measured in the circuit configuration that was developed, but earlier measurements on single SQUIDs during the development of the process point to an 80 % yield.

From previous measurements on similar SQUIDs,we determined the temperature dependance of ß, and the transition temperature of the devices. Some of these devices operated over 77 K, resulting in measurable phase shifts above 77 K.

2.4 HTS Circuit Design- Monolithic Implementation

The first step toward a monolithic implementation of the HTSSE phase shifter incorporated one SQUID device at the center of the resonator. Early measurements on this design determined that the microstrip resonator coupling gap (8 mils) was too large, so the coupling was too weak.

A new mask was made with a stronger coupling (a smaller gap of 4 mils). To increase the phase shift, a total of 40 SQUIDs were incorporated into the resonator. The length of the resonator was increased to insure that the device operated in the NRL test frequency range. The microstrip linewidth is 5.5 mils, the SQUID inductance hole is 40 µm square, the microbridge width was designed for 2 µm, and the step edge trough was 2 µm wide and 150 nm deep.

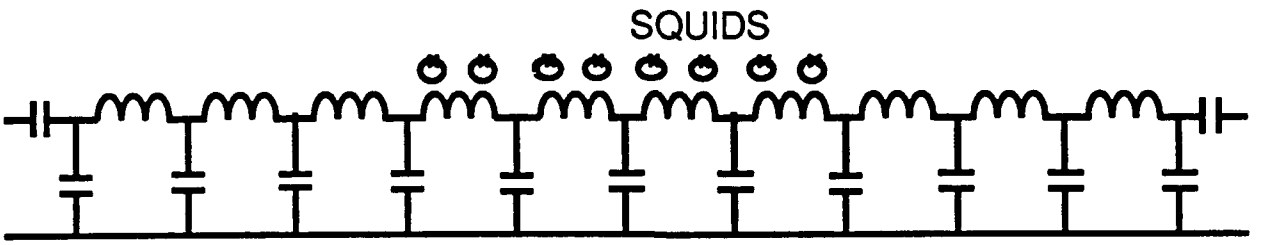

Fig. 2.4-1 Simple L and C model of circuit with many SQUIDs coupled to the resonator.

A simple model of the circuit using lumped elements, shown in Fig. 2.4-1, can be used to model the performance of the phase shifter. The coupling gap was chosen so that the resonator loaded Q was about 200. The layout of the HTS resonator (Fig. 2.4-2), shows only a microstrip resonator because the HTS SQUIDs are too small to be seen on this scale. A photograph of the HTS SQUIDs imbedded in the microstrip resonator is shown in Fig. 2.4-3. Finally, a photograph of an HTS SQUID imbedded in the microstrip resonator shows the microbridge and the step edge groove.

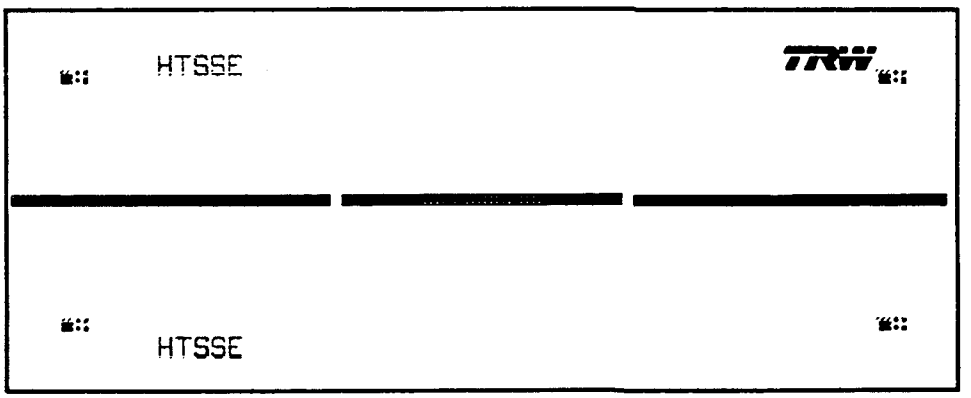

Fig. 2.4-2 Layout of the HTS resonator, the HTS SQUIDs are too small to be seen on this scale.

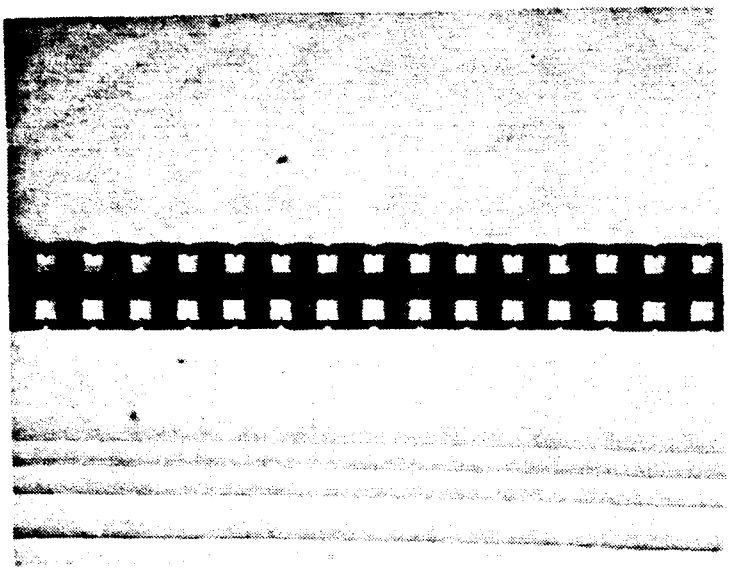

Fig. 2.4-3 Photograph of the HTS SQUIDs imbedded in the microstrip resonator, the SQUID inductance holes are barely visible, and the microbridges are too small to be seen on this scale.

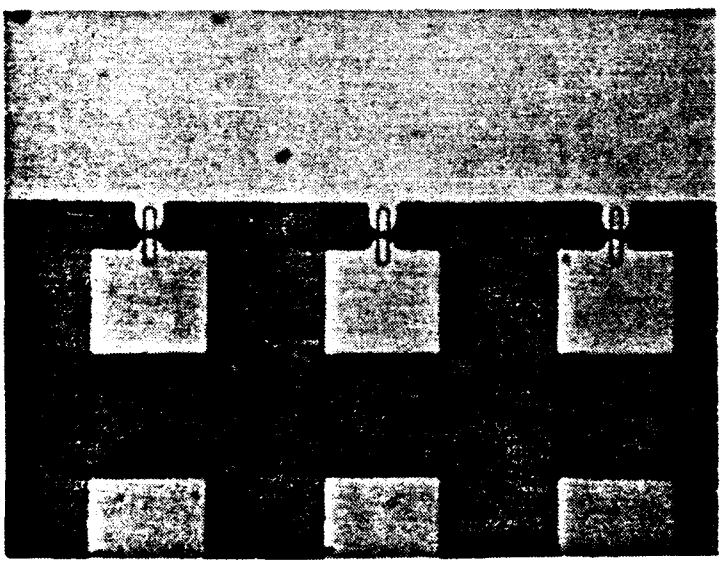

Fig. 2.4-4 Photograph of an HTS SQUID imbedded in the microstrip resonator, and the microbridge and the step edge groove can be seen.

2.5 Component Assembly and Housing Design

A number of parts were needed to make the HTS phase shifter. Fig. 2.5-1 shows the main housing, the cover, an HTS chip, hermetic filter feed troughs, and the coil cover before assembly. Figure 2.5-2 shows the assembled HTS phase shifter.

The housing design is similar to the devices delivered in June. The most substantial change was the use of brass instead of Kovar. Kovar has a high magnetic permeability, and a (potentially) high internal magnetization that is detrimental to SQUID devices. Brass has a reasonable coefficient of thermal expansion and conductivity, and a higher electrical resistance than copper. The higher electrical resistance of brass (compared to copper) facilitates the welding of hermetic seals.

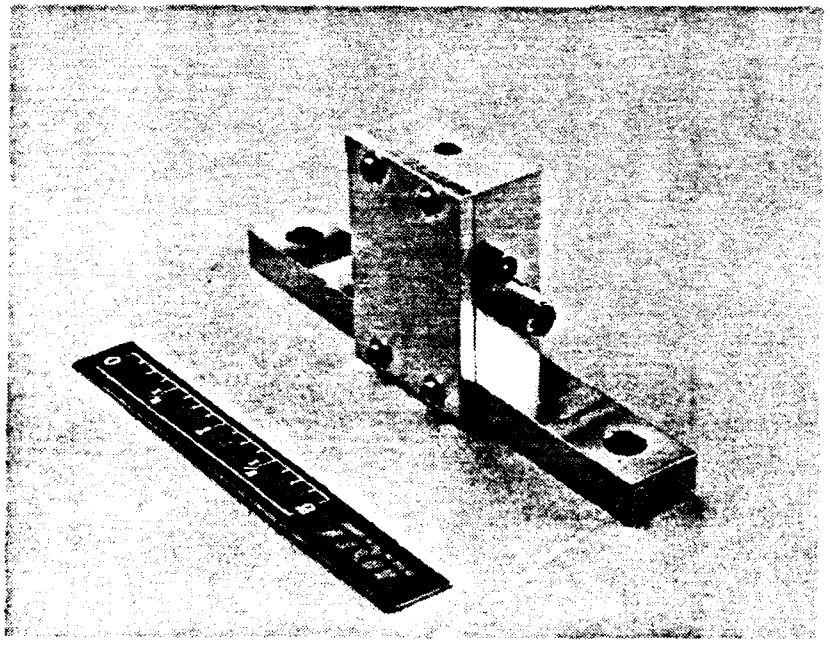

Fig. 2.5-1 Unassembled phase shifter, showing main housing, cover, mounted microwave circuit (in main housing), extra microwave circuit (near housing), and coil holder.

A second modification changed the package dimensions to agree more fully with the NRL outline. At the same time the internal volume of the package was increased to force an internal parasitic resonance to lower frequencies. The resulting resonance was lower, but still in the NRL range of test frequencies.

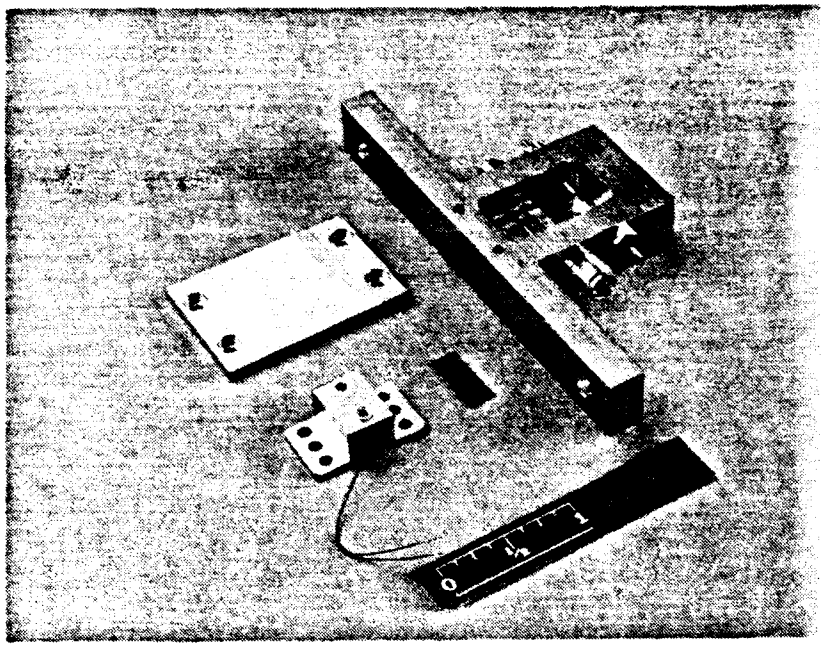

Fig. 2.5-2 Assembled phase shifter.

3.0 Phase Shifter Performance

This section describes the performance of the phase shifter. Plots of phase shift vs. control current at 16 K and 77 K are included. Plots of insertion loss vs. frequency show a shift in frequency indicative of true time delay properties. Plots of phase shift and Q vs. temperature show the operating range of the device. SQUID related effects were observed, as shown by the magnetic field dependence of the phase shift response.

3.1 Phase Shift vs. Control Current

The HTSSE phase shifter operates by controlling the flux through SQUID inductance loops. A 12 turn loop placed above the resonator changes the flux in the present design, but a dc current can be used in future, non-resonant designs. Figure 3.1-1 shows the sinusoidal change in phase produced by a sweep field. Increasing the sweep size increases the number of sinusoidal cycles, and changing the dc magnetic field shifts the peaks, as section 3.5 shows.

The flux through the SQUID inductance lops determines the average inductance of the SQUID. This inductance couples to the microstrip line, contributing to the phase velocity of the transmission line. Changing the flux through the inductance hole changes the average phase velocity, thereby causing a phase shift. Figure 31.-2 shows that the microstrip resonance is actually shifted by the application of the external control field.

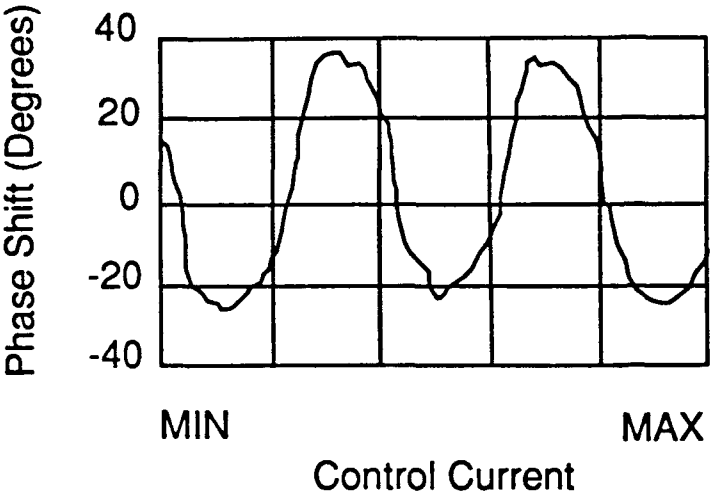

Fig. 3.1-1 Plot of phase vs. frequency and applied control current

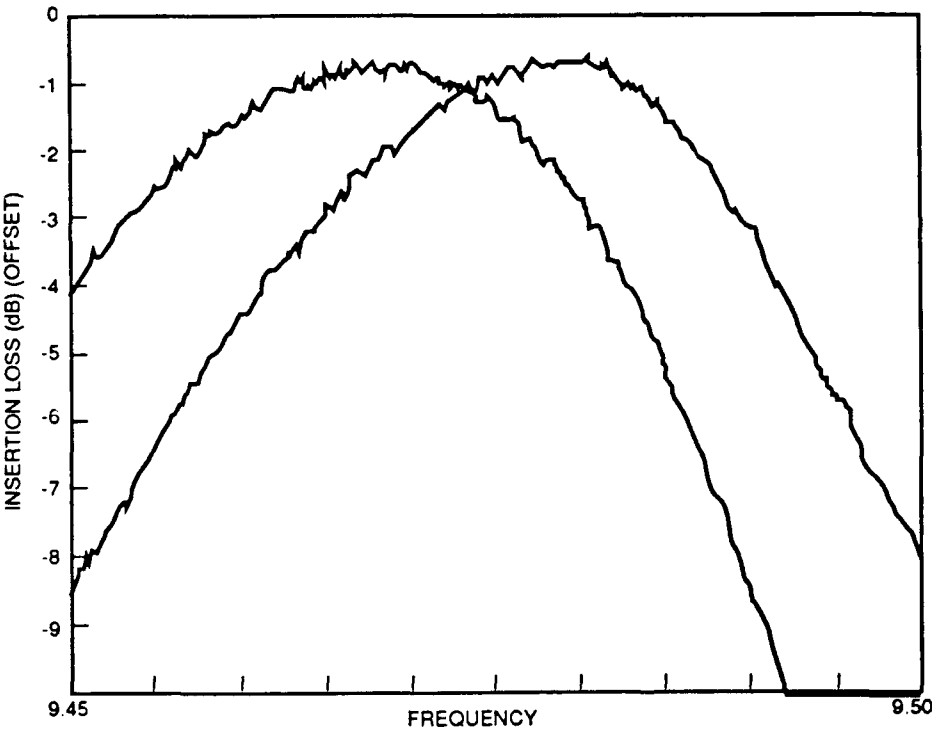

Fig. 3.1-2 Insertion loss at two control current settings showing shift in resonant frequency.

Typically, a phase shifter is used with discrete phase steps of 180, 90,45, 22.5, ... step sizes. Figure 3.1-3 shows the phase and amplitude for a discrete phase change. Due to limitations in the present circuit design, no attempt was made to determine the

switching speed, however, Fig. 3.1-3 shows that it was faster than one millisecond. This device's switching time is limited by the inductance of the control loop and the eddy currents that are formed in the metal of the housing. A current controlled device will be even faster.

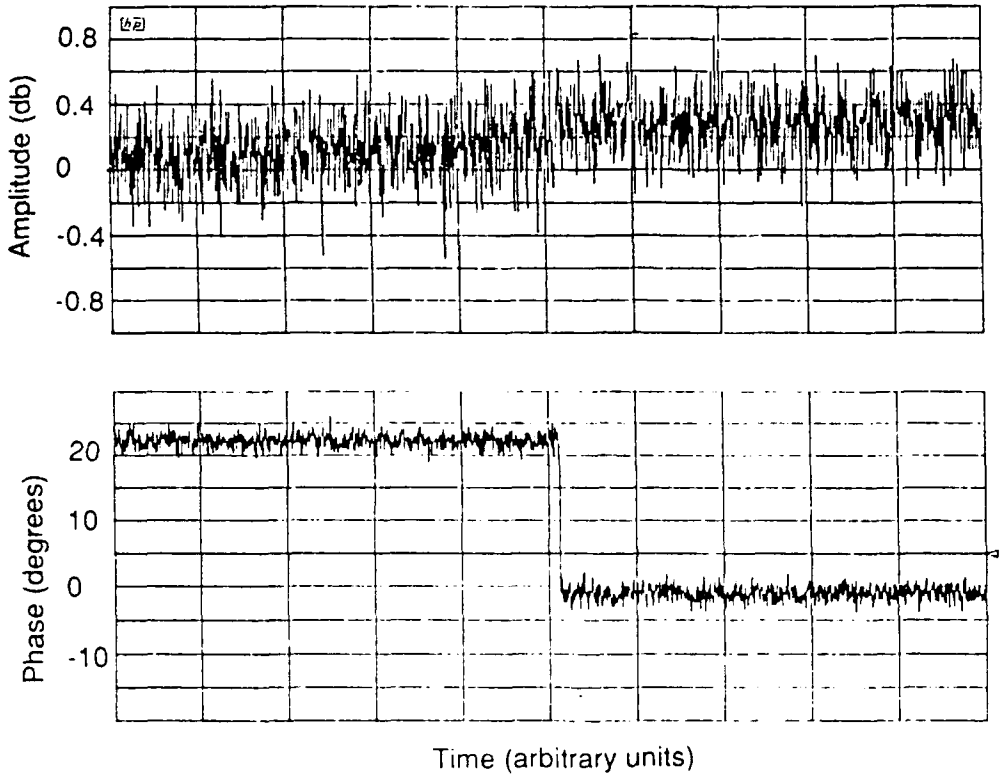

Fig. 3.1-3 Phase shift for two settings of control current. A 22.5 degree phase shift was obtained with less that 0.2 dB variation in insertion loss. This data was obtained from housing DD at 16 K.

3.2 Phase Shift vs. Temperature

The measured phase shift changes with temperature. The temperature dependance of the Q and the resonance frequency (Figs. 3.2-1 and 2) are qualitatively related to the measured phase shifts (Fig. 3.2-3).

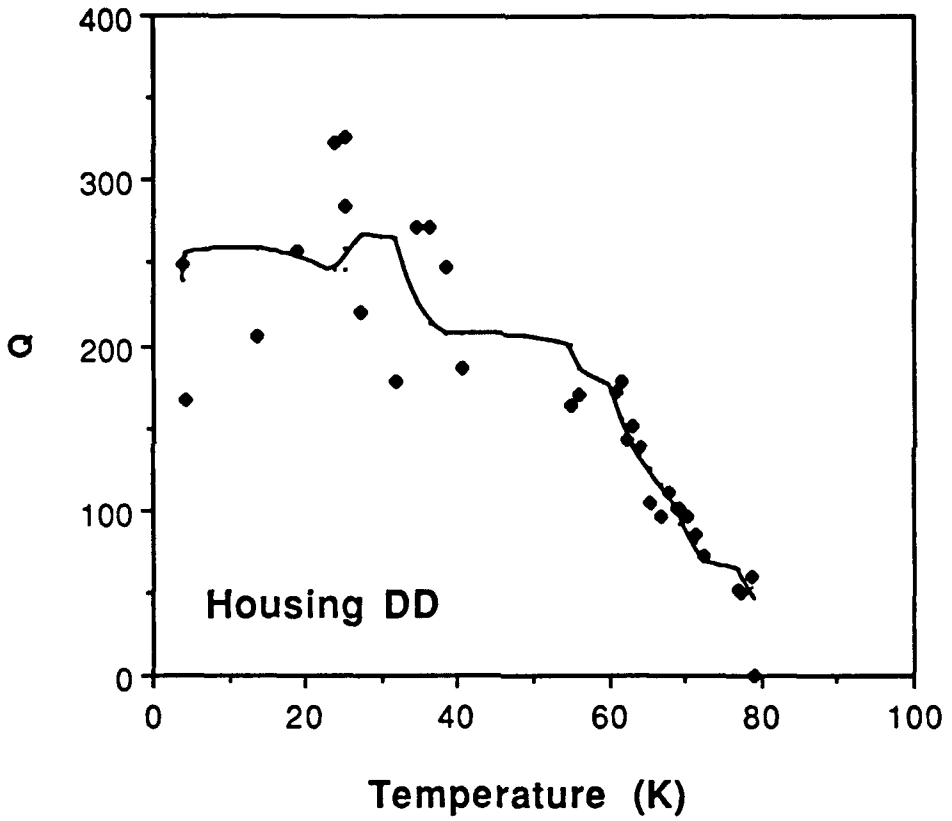

Fig 3.2-1 Measured Q-value vs. temperature. The solid line is a 5 point running average of the data to aid the data analysis.

The Q vs. temperature plot is noisy because small, low frequency, magnetic fields perturbed the insertion loss measurements. The resonance frequency vs. temperature plots were less sensitive to the magnetic fields. Both of these measurements were performed outside of a magnetic shield because the switches and through calibration were too large to fit in a shielded cylinder. The frequency shift vs. temperature data

provided similar plots for all devices and were much more reproducible from run to run.

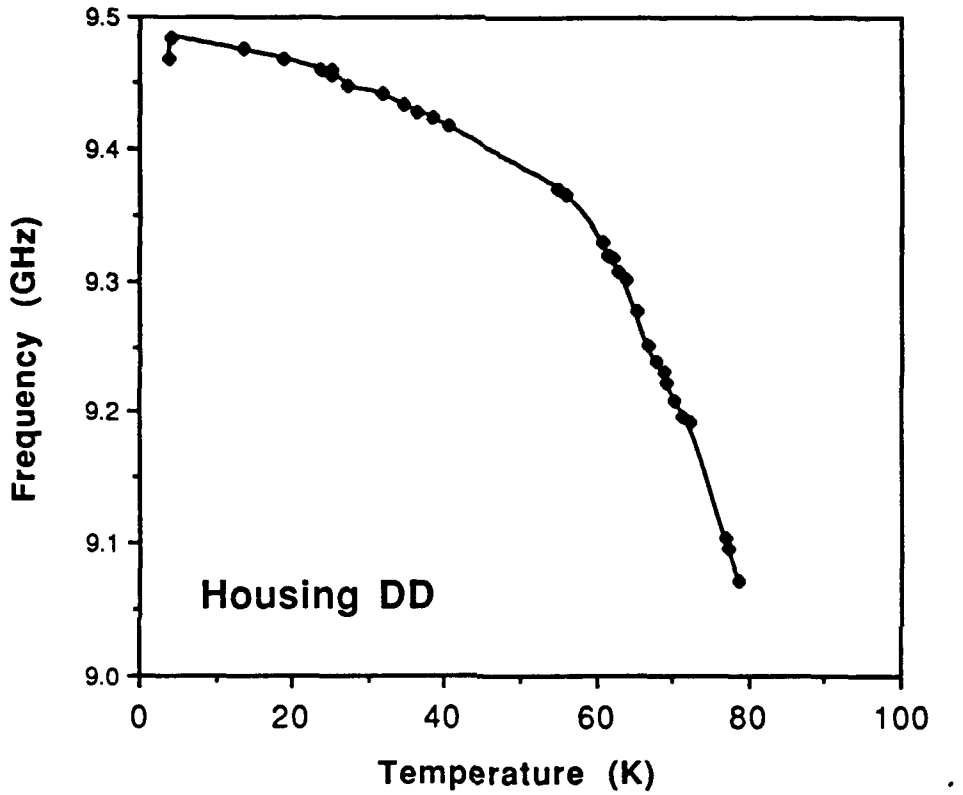

Fig. 3.2-2 Plot of resonance frequency vs. temperature. The solid line connects data points.

The phase shift was measured over temperature for the different devices. Generally, the phase shift was largest at low temperatures. At higher temperatures, the phase shift gets smaller. The curve follows the general trend of the Q vs. temperature shown in Fig. 3.2-1.

Two possible contributions to the decline in the phase shift at higher temperatures are the decline in the Q and the reduction in the SQUID ß-parameter. The Q of the resonator enhances the measured phase shift, so a reduction in Q reduces the measured phase shift. The magnitude of the phase shift is proportional to ß. The ß of a SQUID is proportional to the critical current of the Josephson device, so as the

critical current declines as Tc is approached, the ß declines, and the phase shift gets smaller.

The present state-of-the-art microbridges are not perfect Josephson elements; there are some irregularities in the response to a magnetic field, resulting in a range of values for the critical current as a function of applied field. Hence the error bars in Fig. 3.2-3 for the phase shift reflect the different values obtained at different fields. The variation in phase shift over a single flux quantum is much smaller than the error bars suggest.

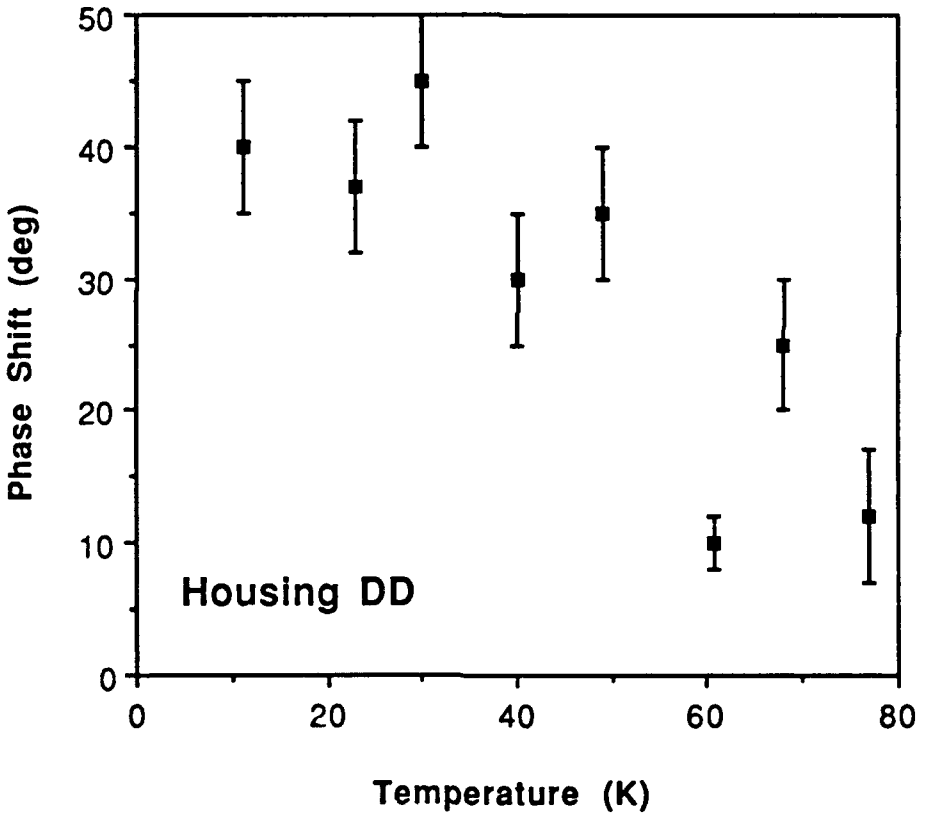

Fig. 3.2-3 Plot of measured peak-to-peak phase shift vs. temperature.
The error bars show the variation between different flux quantum transitions.

3.3 Phase Shift vs. Power

The HTS phase shifters show pronounced power dependances. Below power levels of -65 dBm incident to the devices, the peak-to-peak phase shift is nearly constant. Measurements at lower powers are difficult to perform because the noise floor of the system dominates.

The steep decline in peak-to-peak phase shift followed by a slow one was observed in a few of the devices- it may be a real effect. The frequency dependance of the resonance is shown, but seems uncorrelated to the phase shift data.

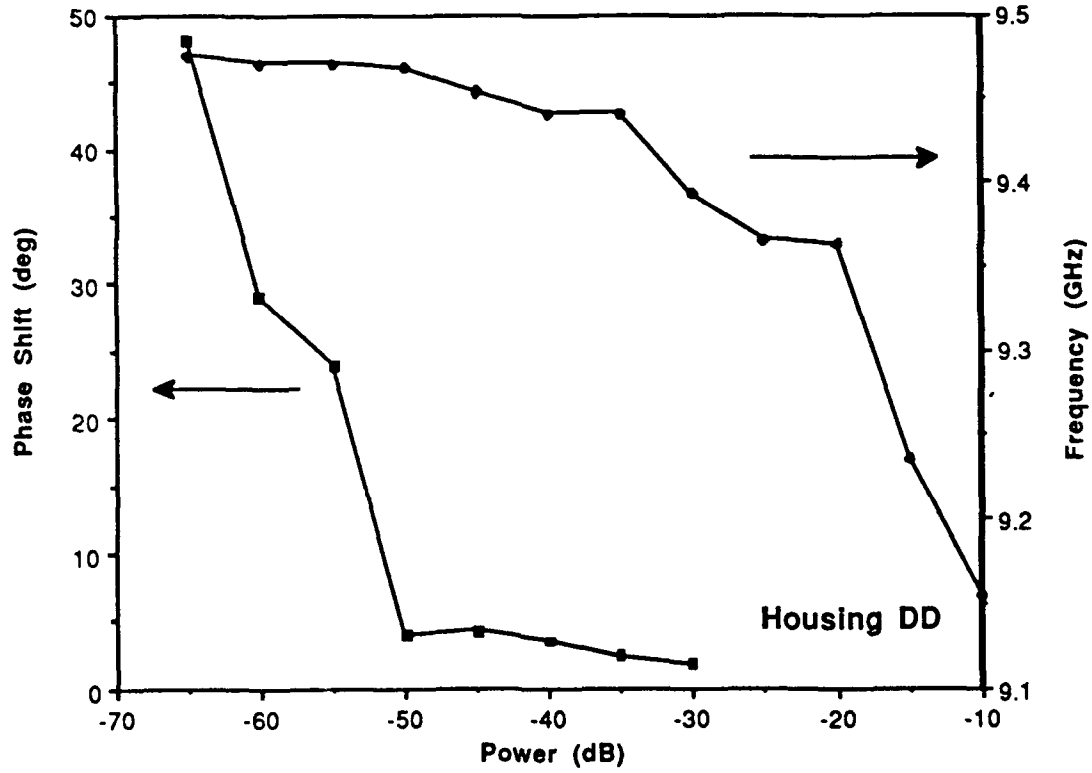

Fig. 3.3-1 Phase shift and frequency shift vs. applied power.

3.4 Demonstration of Phase Shift Above 77 K

A number of the phase shifters operated at 77 K. As an example, Figure 3.4-1 shows the response of one of the housings at 77 K; the observed phase shift was 20 degrees at 77 K. As shown in Figure 3.2-3, the phase shift typically decreases with increasing temperature.

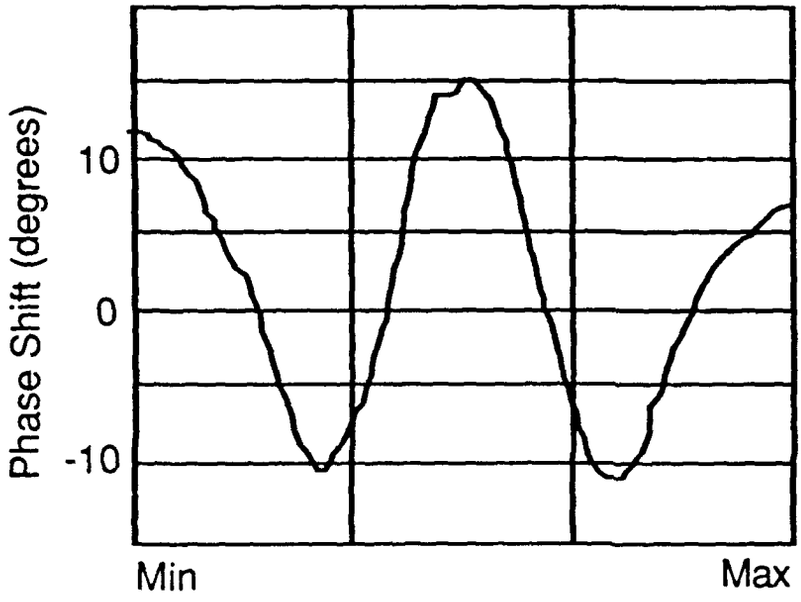

Fig. 3.4-1 Phase shift vs. control current at 77 K This data is from device AA. This trace was averaged 16 times to improve the signal to noise.

3.5 Demonstration of SQUID Related Behavior

It is possible to obtain periodic phase shifts which do not depend on the flux quantas. This section shows that the observed phase shifts are due to SQUID responses, and not some spurious response.

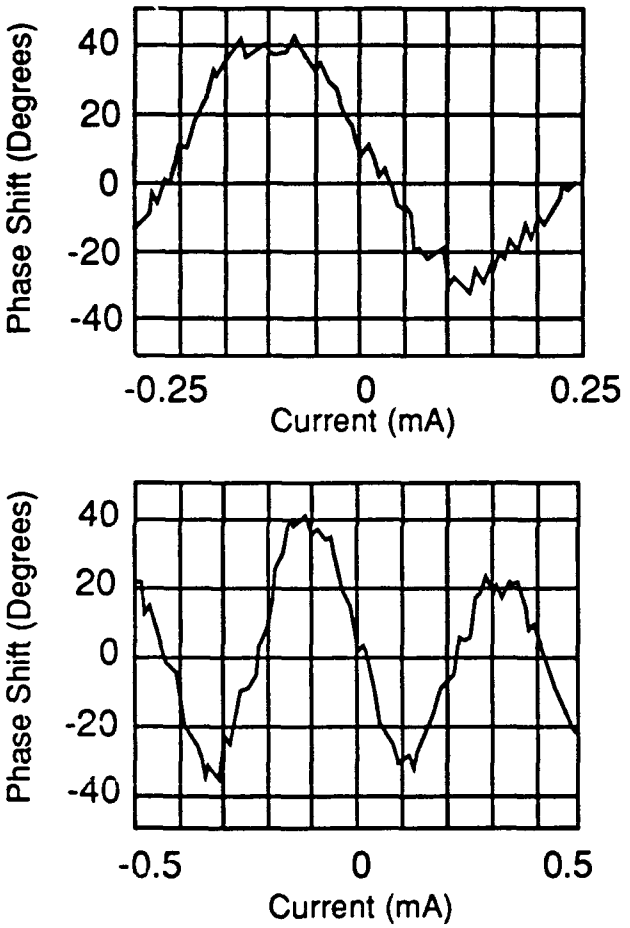

Fig.3.5-1 a) Phase shift vs. applied field for a small control signal ramp, b) for a larger control signal ramp (about twice the size).

Two properties separate SQUID related behavior from other kinetic inductance effects such as heating. The first is the flux quanta related periodicity, and the second is the dc offset response. The each flux quantum through the inductance loop causes the periodic response of a SQUID. Hence, increasing the size of a the applied magnetic field increases the number of phase cycles. Doubling the size of the applied magnetic

field doubles the number of flux quanta through the SQUID inductance loop, as Fig. 3.5-1 shows.

When the applied dc magnetic field is changed, the SQUID pattern shifts by that amount. Figure 3.5-2 shows the effect of a change in the dc control current. These three plots demonstrate that SQUID related behavior was observed, as opposed to some other effect such as heating.

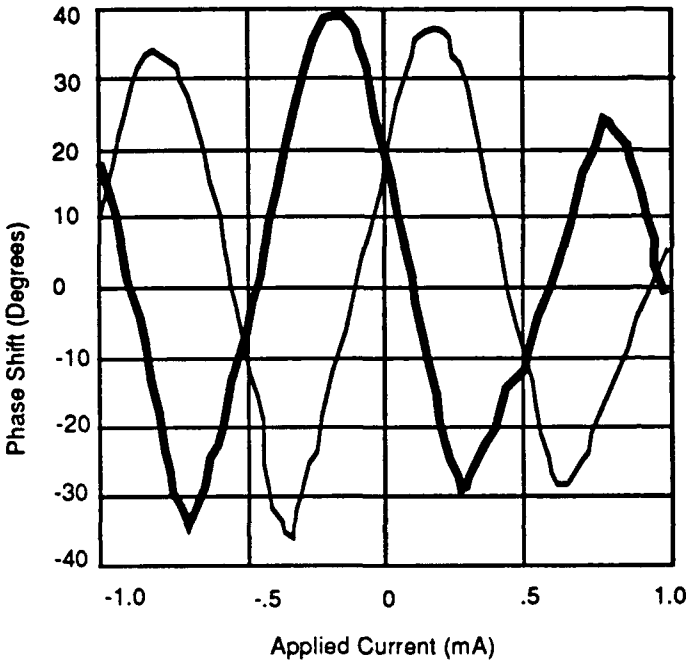

Fig.3.5-1 Phase shift vs. applied field. The bold line is for one dc value; the thin line is for a larger dc value (about 1/4 flux quantum larger).

4.0 Effects of Aging

TRW delivered five resonators to NRL in June 1990. Two additional resonators were fabricated, but they had lower Q values than the devices that were delivered. We repeated our measurements of the one of these devices. These devices were stored at room temperature in a laboratory environment.

Within the measurement uncertainty, we did not observe any change in the performance of the device that was measured in June 1990 (Fig. 4-1) and later in February 1991 (Fig. 4-2). The Q and the transition temperature remained unchanged. The changes in Figs. 4-1 and 4-2 are due more to our improved measuring capability, than to changes in the film properties.

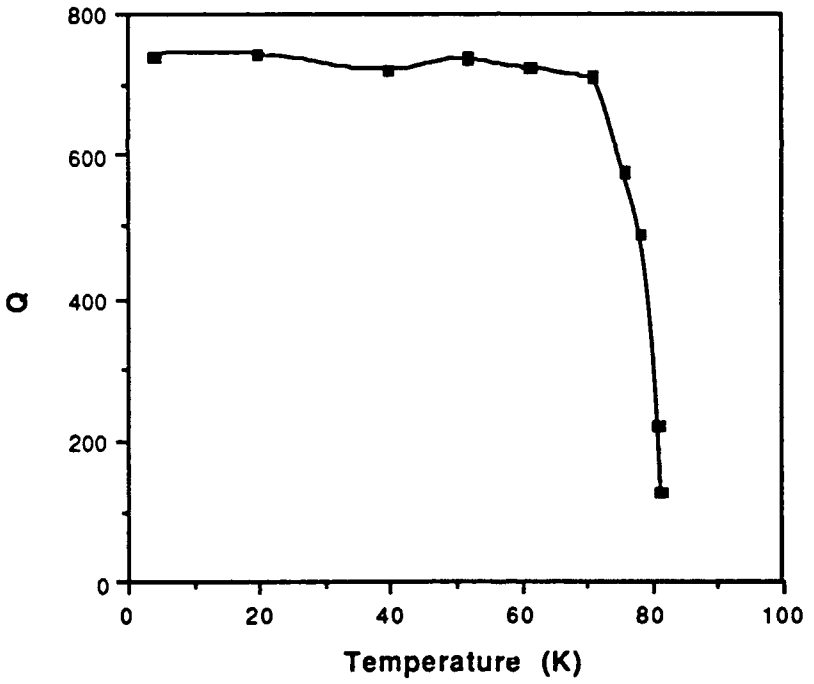

Fig.4-1 Measured Q vs. T for device 4 in June 1990.

In the months following the original delivery, we refined our power dependance measuring capability, and we observed a power dependance to the resonator Q in the

device at high powers. The Q was reduced from 1050 at -55 dBm to 900 at -10 dBm incident power.

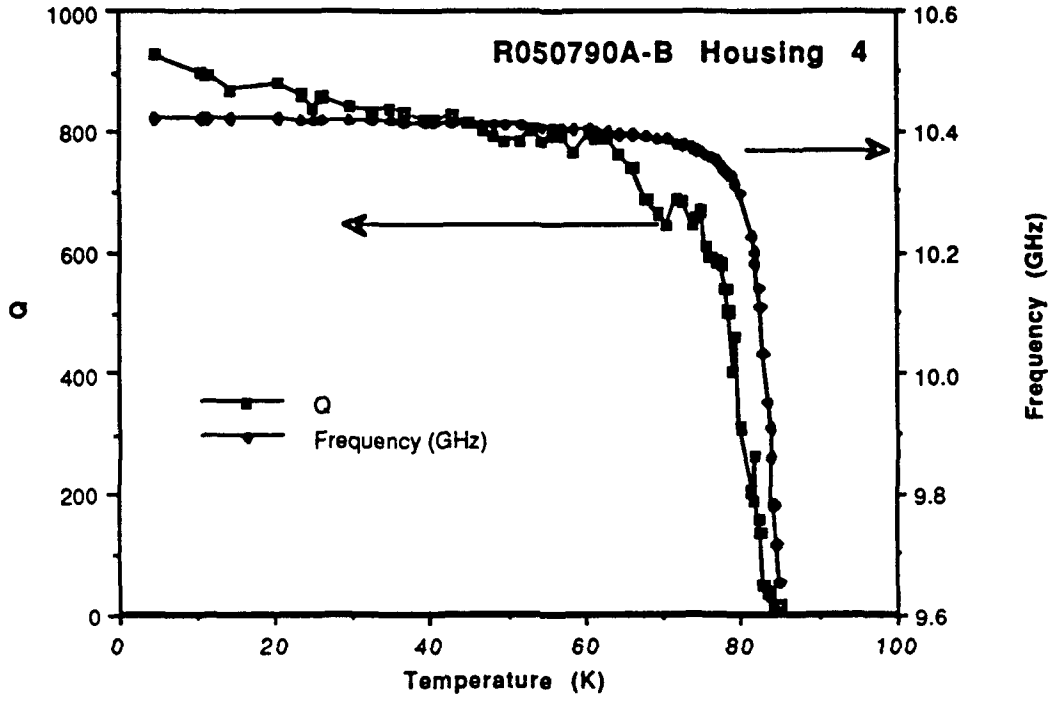

Fig.4-2 Measured Q vs. T for device 4 in February 1991. Both the Q and the resonance frequency are shown.

5.0 Measurement Procedure

The HTS phase shifters were measured using the block diagram of Fig. 5-1. The external trigger feature of the HP 8720 network analyzer was very useful for the phase shift measurements. For the Q measurements, the HP 8720 collected the insertion loss data and a built-in Q measuring feature speeded the computerized data acquisition.

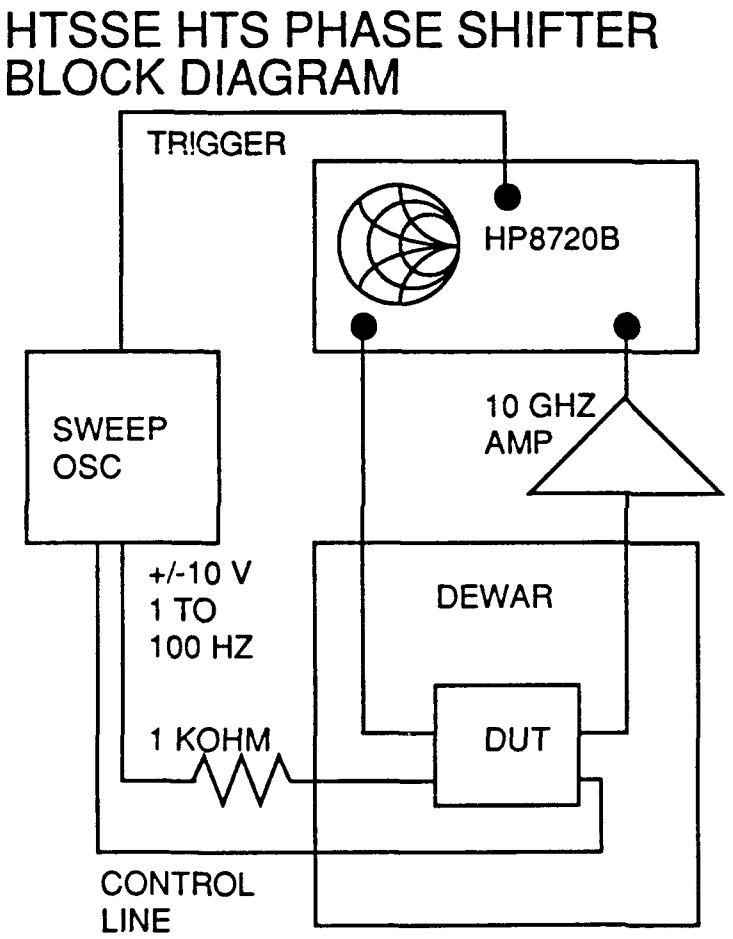

Fig. 5-1 Block diagram for HTS phase shifter measurements.

A low frequency sweep oscillator (1 to 100 Hz) provided a voltage over a 1 Kohm resistor to provide the current bias for the control coil in the housing. A trigger signal was sent to the HP 8720 Vector Network Analyzer. The 10 GHz signal (typically at -50 dBm) was fed to the device, followed by a 27 dB amplifier (to raise the signal above the noise floor). The device under test (DUT) had 3-dB pads on the input and output to reduce the effects of standing waves along the long coax lines between the DUT and

the network analyzer. For the phase shifter measurements, a magnetic shield was placed around the device under test.

When the insertion loss vs. frequency was measured, a pair of cryogenically cooled switches were employed with a through-line standard to allow an accurate calibration at all temperatures. The switches and through calibration were too large to fit in a cylindrical magnetic shield.